Supporting Information: Regenerated and Reformed Gold and Titanium Dioxide Quantum Dots from Waste for Sustainable and Efficient Environmental Monitoring

Zain Ul Abideen,* Rasoul Khayyam Nekouei, Mohsen Hajian-Foroushani, Samane Maroufi, Farshid Pahlevani, and Veena Sahajwalla

Centre for Sustainable Materials Research and Technology, SMaRT@UNSW, School of Materials Science and Engineering, UNSW Sydney, NSW 2052, Australia

E-mail: zain.abideen@unsw.edu.au

Table S1: Elemental composition of commercial and recycled TiO_2 materials determined by XRF and ICP-OES.

Element	**Technique**	**Sample**	**Content (wt%)**
TiO_2	XRF	Commercial TiO_2	98.44
TiO_2	XRF	Recycled R-Au-TiO_2 QDs	83.32
Ti	ICP-OES	Recycled R-Au-TiO_2 QDs	0.553
Ti	ICP-OES	Commercial TiO_2	0.035
Au	ICP-OES	Recycled R-Au-TiO_2 QDs	0.239

Note: TiO_2 values from XRF represent oxide form; Ti values from ICP-OES represent elemental form. Au was detected only in the recycled sample. All values are based on independently prepared samples and rounded to three decimal places.

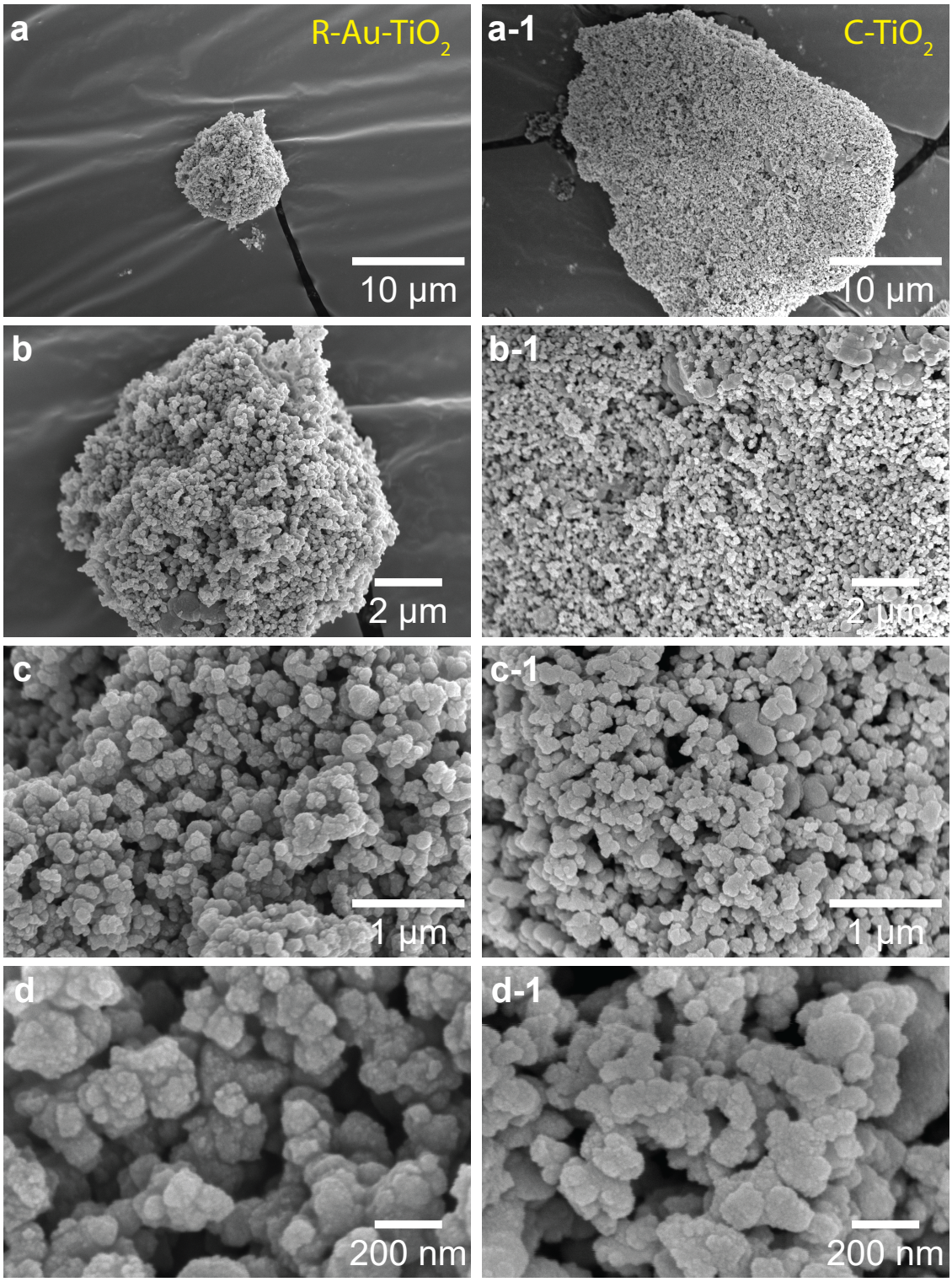

Figure S1: SEM images at different magnifications comparing reformed Au-TiO_2 (R-Au-TiO_2) hybrid quantum dots (QDs) from waste and commercial TiO_2 nanoparticles (C-TiO_2). (a) and (a-1) show overall structures at 10 μm scale. (b) and (b-1) provide closer views at 2 μm scale. (c) and (c-1) further zoom in at 1 μm scale. (d) and (d-1) reveal nanoscale features at 200 nm scale, highlighting the similar agglomerated morphology and detailed structural characteristics of both samples.

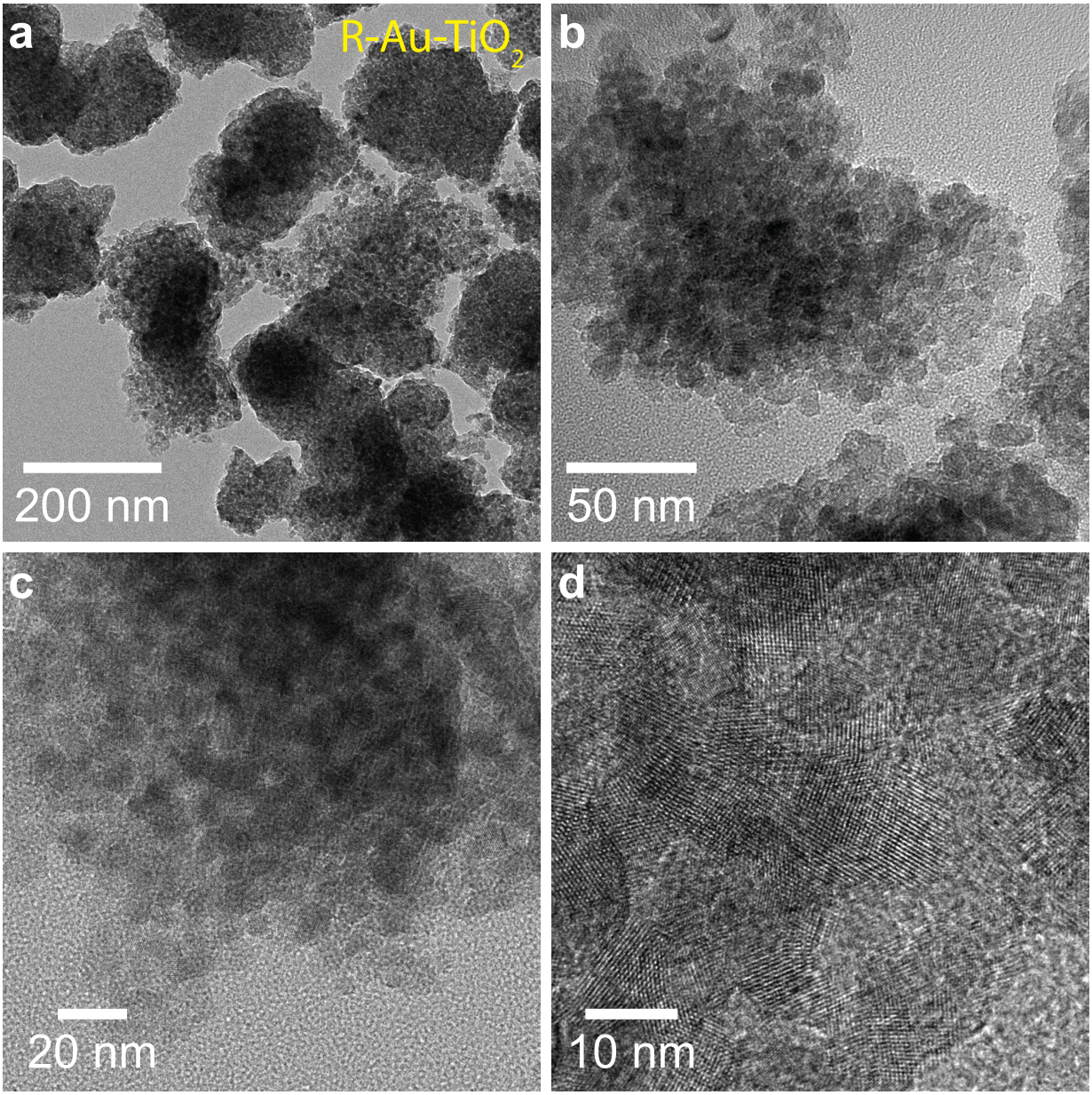

Figure S2: TEM images of R-Au-TiO_2 QDs at varying magnifications. (a) shows the overall morphology at 200 nm scale (b) provides a closer view at 50 nm scale (c) further zooms in at 20 nm scale, and (d) reveals lattice fringes at the nanoscale (10 nm), highlighting the well-dispersed and uniform size distribution, along with the high crystallinity of the R-Au-TiO_2 QDs.

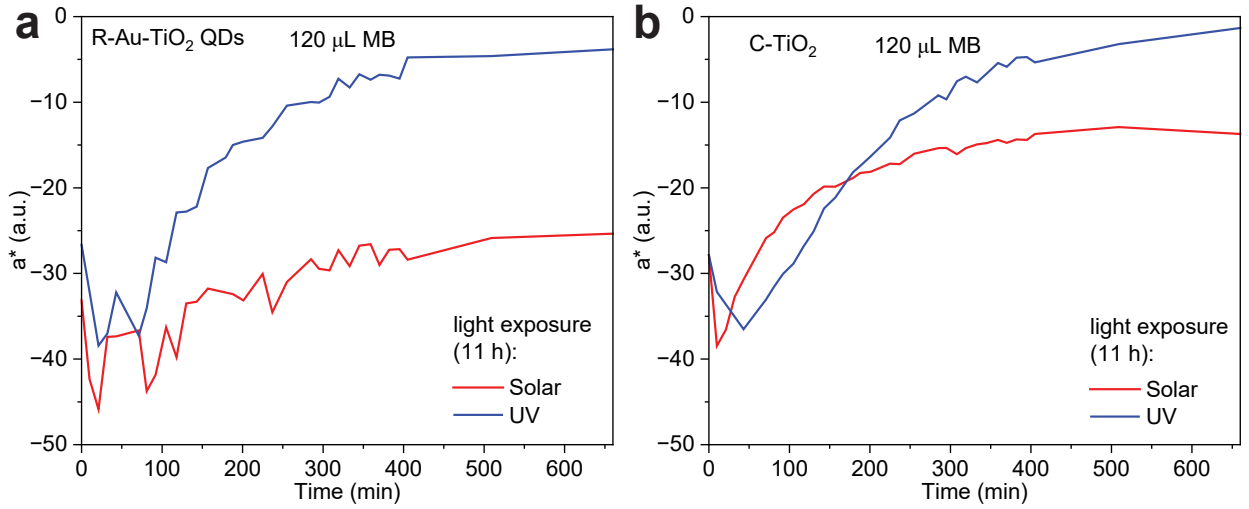

Figure S3: The a* component of the CIELAB colour system for (a) R-Au-TiO_2 QDs and (b) C-TiO_2 nanoparticles as a function of time during 11 hours of exposure to the solar simulator and UV light at 254 nm. The plots illustrate the colourimetric changes in the sensors, with initial a* values indicating a greenish tint due to the presence of methylene blue (MB). As MB degrades over time, the a* values increase, reflecting a shift towards the red spectrum. This change is more pronounced in R-Au-TiO_2 QDs under UV light, indicating more efficient degradation of MB compared to C-TiO_2.

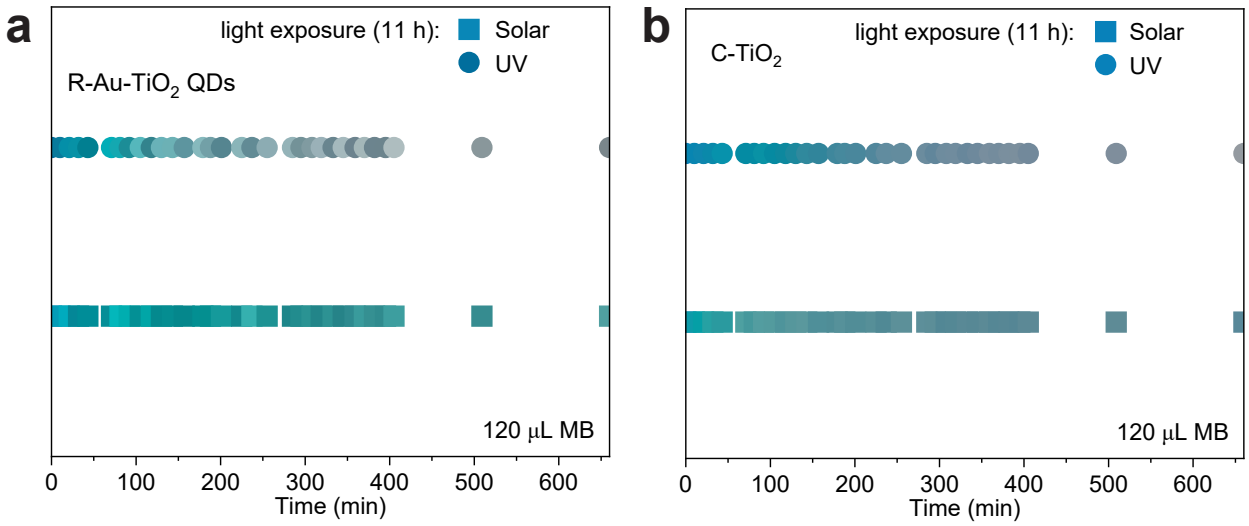

Figure S4: Visual representation of the colour changes in (a) R-Au-TiO_2 QDs and (b) C-TiO_2 nanoparticles films during 11 hours of exposure to solar simulator and UV light at 254 nm. The colour transitions from blue-green to yellow indicate the degradation of MB over time, with more pronounced changes observed under UV light for R-Au-TiO_2 QDs, reflecting their superior photocatalytic performance compared to C-TiO_2.

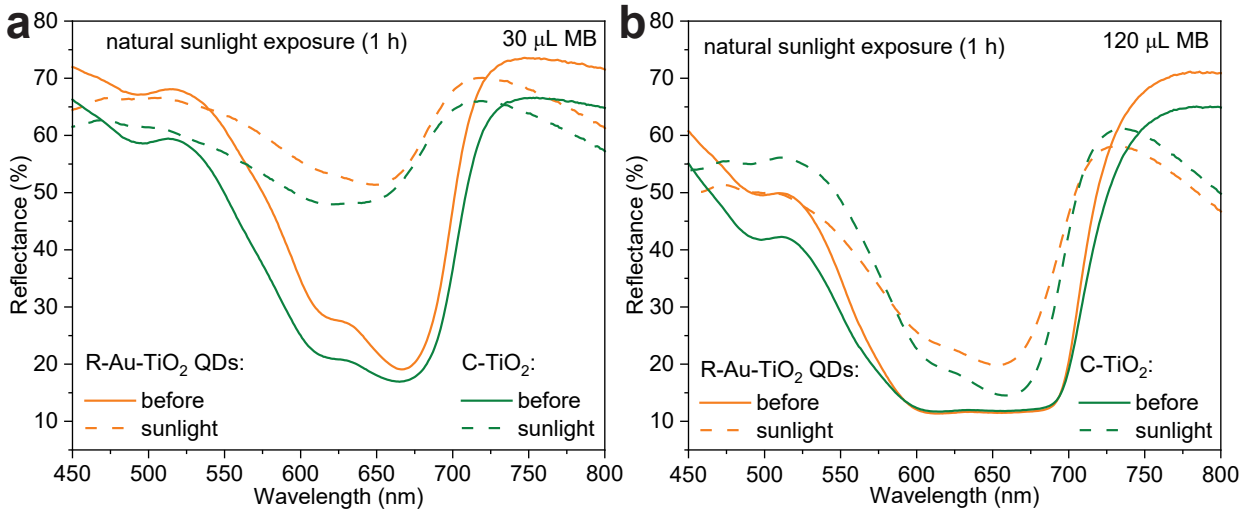

Figure S5: Reflectance spectra of R-Au-TiO_2 QDs and C-TiO_2 nanoparticles before and after 1 hour of natural sunlight exposure for films containing (a) 30 μL and (b) 120 μL of MB. The solid lines represent the spectra before exposure, while the dashed lines represent the spectra after sunlight exposure. The results show a significant decrease in MB absorption in both samples after exposure, indicated by the reduced absorption peak around 650-700 nm, with R-Au-TiO_2 QDs demonstrating a more pronounced change, reflecting their superior photocatalytic performance under natural sunlight conditions.

Table S2: Overview of various TiO_2-based materials used for photocatalytic degradation of MB under different light sources. The R-Au-TiO_2 QDs, derived from waste and used in this study, demonstrate comparable or superior photocatalytic performance under UV (254 nm), solar simulator, and natural sunlight conditions, with particle sizes less than 10 nm. This performance is benchmarked against a variety of commercial and synthesized TiO_2 materials from the literature.

TiO_2 preparation	**TiO_2 source**	**Substrate**	**Methylene blue concentrations**	**Film thickness**	**Film deposition method**	**Light source**	**Particle size**	**Key performance indicator**	**Ref.**
R-Au-TiO_2 QDs	metallurgical waste	Glass and aluminium foil	30 μL and 120 μL	200 μm	Doctor blade	UV, solar simulator, and natural sunlight	< 10 nm	Rate constant: 0.029 min^{-1}	This work
Commercial TiO_2	Commercial TiO_2	-	1000 ppm	-	-	UV	120-180 nm	Rate constant: 0.1192 min^{-1}	S1
Hydrothermal	$TiCl_4$	-	10 mg L^{-1}	-	-	UV (365 nm, 6W)	4.5 nm	Rate constant: 0.018 min^{-1}	S2
Cu-doped TiO_2 (sputtering)	Pure Ti source	glass	30 mg L^{-1}	200 nm	DC sputtering	UV	-	-	S3
TiO_2/Au	Commercial TiO_2 nanoparticle	-	0.1 mg mL^{-1}	-	-	Chemical degradation	Au (10 nm), TiO_2 (21 nm)	Degradation rate: 79-87%	S4
Sol-gel (Fe_2TiO_5)	Commercial precursors	-	1000 mg L^{-1}	-	-	Natural sunlight	49.7 nm	Rate constant: 0.015 min^{-1}	S5
Sol-gel (TiO_2, Au-TiO_2)	Commercial precursors	quartz glass	1.16 x 10^{-5} M	200-250 nm	Dip coating	UV	Au (13 nm), TiO_2 (25-29 nm)	-	S6
Commercial TiO_2	Commercial P25 TiO_2	-	500 ppm	-	-	UV	25 nm	-	S7
Commercial TiO_2	Commercial TiO_2	-	5, 10, 15, 20 mg L^{-1}	-	-	UV (364 nm)	10-200 nm	Degradation efficiency: 90%	S8
Commercial TiO_2	Commercial TiO_2	-	10 ppm	-	-	UV	25 nm	Rate constant: 0.055 min^{-1}	S9
solvent-thermal method (TiO_2-PRGO)	Commercial precursors	-	10 mg L^{-1}	-	-	Solar simulator	9.85-11.7 nm	Rate constant: 0.0275 min^{-1}	S10
Commercial TiO_2	Commercial TiO_2	soda lime glass	10 mg L^{-1}	6 µm	Doctor blade method	UV	25 nm	Rate constant: 0.15 min^{-1}	S11
Sol-gel (TiO_2/ graphene oxide)	Commercial precursors	-	5-25 mg L^{-1}	-	-	UV	-	-	S12
Sol-gel (TiO_2)	Commercial precursors	glass substrate	1 x 10^{-6} M	220 nm	Spin coating	Visible light	54-67 nm	Degradation efficiency: 92%	S13
Physical vapor deposition (TiO_2/Nd_2O_3)	Commercial precursors	Si (100)	5 and 20 mg L^{-1}	100 nm	EB-PVD	UV	-	Degradation rate: 72.9%	S14
Hydrothermal (TiO_2)	Commercial precursors	FTO coated glass	5 ppm	-	-	Solar simulator (300-600 nm)	-	Rate constant: 0.00183 min^{-1}	S15

References

(S1) Abdellah, M.; Nosier, S.; El-Shazly, A.; Mubarak, A. Photocatalytic decolorization of methylene blue using TiO2/UV system enhanced by air sparging. *Alexandria Engineering Journal* **2018**, *57*, 3727–3735.

(S2) Azeez, F.; Al-Hetlani, E.; Arafa, M.; Abdelmonem, Y.; Nazeer, A. A.; Amin, M. O.; Madkour, M. The effect of surface charge on photocatalytic degradation of methylene blue dye using chargeable titania nanoparticles. *Scientific Reports* **2018**, *8*, 7104.

(S3) Carvalho, H. W.; Batista, A. P.; Hammer, P.; Ramalho, T. C. Photocatalytic degradation of methylene blue by TiO2-Cu thin films: Theoretical and experimental study. *Journal of Hazardous Materials* **2010**, *184*, 273–280.

(S4) Jinga, L. I.; Popescu-Pelin, G.; Socol, G.; Mocanu, S.; Tudose, M.; Culita, D. C.; Kuncser, A.; Ionita, P. Chemical Degradation of Methylene Blue Dye Using TiO2/Au Nanoparticles. *Nanomaterials* **2021**, *11*, 1605.

(S5) Vasiljevic, Z. Z.; Dojcinovic, M. P.; Vujancevic, J. D.; Jankovic-Castvan, I.; Ognjanovic, M.; Tadic, N. B.; Stojadinovic, S.; Brankovic, G. O.; Nikolic, M. V. Photocatalytic degradation of methylene blue under natural sunlight using iron titanate nanoparticles prepared by a modified sol-gel method. *Royal Society Open Science* **2020**, *7*, 200708.

(S6) Yogi, C.; Kojima, K.; Wada, N.; Tokumoto, H.; Takai, T.; Mizoguchi, T.; Tamiaki, H. Photocatalytic degradation of methylene blue by TiO2 film and Au particles-TiO2 composite film. *Thin Solid Films* **2008**, *516*, 5881–5884.

(S7) Xu, C.; Rangaiah, G. P.; Zhao, X. S. Photocatalytic Degradation of Methylene Blue by Titanium Dioxide: Experimental and Modeling Study. *Industrial & Engineering Chemistry Research* **2014**, *53*, 14641–14649.

(S8) Dariani, R.; Esmaeili, A.; Mortezaali, A.; Dehghanpour, S. Photocatalytic reaction and degradation of methylene blue on TiO2 nano-sized particles. *Optik* **2016**, *127*, 7143–7154.

(S9) Tichapondwa, S.; Newman, J.; Kubheka, O. Effect of TiO2 phase on the photocatalytic degradation of methylene blue dye. *Physics and Chemistry of the Earth, Parts A/B/C* **2020**, *118-119*, 102900.

(S10) Peng, Z.; He, Z.; Li, L.; Xiong, L.; Fan, M. Photocatalytic degradation of methylene blue by efficient TiO2-partially reduced graphene oxide composites. *Applied Organometallic Chemistry* **2024**, *38*.

(S11) Duran, F.; Diaz-Uribe, C.; Vallejo, W.; Muñoz-Acevedo, A.; Schott, E.; Zarate, X. Adsorption and Photocatalytic Degradation of Methylene Blue on TiO2 Thin Films Impregnated with Anderson-Evans Al-Polyoxometalates: Experimental and DFT Study. *ACS Omega* **2023**, *8*, 27284–27292.

(S12) Kurniawan, T. A.; Mengting, Z.; Fu, D.; Yeap, S. K.; Othman, M. H. D.; Avtar, R.; Ouyang, T. Functionalizing TiO2 with graphene oxide for enhancing photocatalytic degradation of methylene blue (MB) in contaminated wastewater. *Journal of Environmental Management* **2020**, *270*, 110871.

(S13) Komaraiah, D.; P.Madhukar; Vijayakumar, Y.; Ramana Reddy, M.; Sayanna, R. Photocatalytic degradation study of methylene blue by brookite TiO2 thin film under visible light irradiation. *Materials Today: Proceedings* **2016**, *3*, 3770–3778.

(S14) Liu, G.; Mamat, M.; Baikeli, Y.; Dong, X. Photocatalytic degradation of methylene blue by TiO2/Nd2O3 composite thin films. *Heliyon* **2024**, *10*, e29894.

(S15) Hamed, N. K. A.; Ahmad, M. K.; Hairom, N. H. H.; Faridah, A. B.; Mamat, M. H.; Mohamed, A.; Suriani, A. B.; Soon, C. F.; Fazli, F. I. M.; Mokhtar, S. M.; Shimomura, M. Photocatalytic degradation of methylene blue by flowerlike rutile-phase

TiO2 film grown via hydrothermal method. *Journal of Sol-Gel Science and Technology* **2022**, *102*, 637–648.